

Geometric reconstruction using tracked ultrasound strain imaging

Thomas S. Pheiffer^a, Amber L. Simpson^a, Janet E. Ondrake^a, Michael I. Miga^{a,b,c}

^aVanderbilt University, Department of Biomedical Engineering, Nashville, TN, USA,

^bVanderbilt University Medical Center, Department of Radiology and Radiological Sciences,
Nashville, TN, USA

^cVanderbilt University Medical Center, Department of Neurological Surgery, Nashville, TN, USA,

ABSTRACT

The accurate identification of tumor margins during neurosurgery is a primary concern for the surgeon in order to maximize resection of malignant tissue while preserving normal function. The use of preoperative imaging for guidance is standard of care, but tumor margins are not always clear even when contrast agents are used, and so margins are often determined intraoperatively by visual and tactile feedback. Ultrasound strain imaging creates a quantitative representation of tissue stiffness which can be used in real-time. The information offered by strain imaging can be placed within a conventional image-guidance workflow by tracking the ultrasound probe and calibrating the image plane, which facilitates interpretation of the data by placing it within a common coordinate space with preoperative imaging. Tumor geometry in strain imaging is then directly comparable to the geometry in preoperative imaging. This paper presents a tracked ultrasound strain imaging system capable of co-registering with preoperative tomograms and also of reconstructing a 3D surface using the border of the strain lesion. In a preliminary study using four phantoms with subsurface tumors, tracked strain imaging was registered to preoperative image volumes and then tumor surfaces were reconstructed using contours extracted from strain image slices. The volumes of the phantom tumors reconstructed from tracked strain imaging were approximately between 1.5 to 2.4 cm³, which was similar to the CT volumes of 1.0 to 2.3 cm³. Future work will be done to robustly characterize the reconstruction accuracy of the system.

Keywords: ultrasound, strain imaging, tracking, neurosurgery

1. PURPOSE

Image-guided neurosurgical procedures largely rely on the premise that the tumor can be clearly demarcated in preoperative tomograms, but this is not always possible with gliomas. The tumor boundaries seen in image volumes are often not in agreement with histological examination of surrounding tissue. It has been shown that in both contrast-enhanced computed tomography (CT)¹ and magnetic resonance (MR) scans², cancer cells can infiltrate far beyond the region of high contrast uptake which defines the tumor boundary in these imaging modalities. It is widely recognized in the medical community that most tumors commonly have significantly different mechanical properties than the surrounding soft tissue. The biological basis for this effect is due to changes in tissue composition, such as varied expression of collagen and greater numbers of fibroblasts^{3,4}. The contrast in mechanical properties is an important tactile cue in guiding the surgeon during resection. Technology which leverages this mechanism, such as ultrasound strain imaging, can potentially assist in identification of cancerous tissue during surgery.

Strain imaging employs a combination of image/signal processing and measurements of the physical deformation of tissue to create a relative representation of the mechanical strength of structures inside the organ of interest^{5,6}. The central premise of this work is that strain imaging can detect margins that are otherwise undetectable in contrast-enhanced tomograms, and that these margins should complement conventional contrast mechanisms, given the link between biomechanical changes and pathology. It would be significantly helpful to establish a clear understanding of the accuracy with which a strain imaging system can detect lesion boundaries. This work presents an analysis of the

ability of strain imaging to characterize a target shape, by placing all of the strain images within a consistent spatial and temporal context via 3D tracking.

1.1 Novel Contributions to be Presented

In the recent literature, several groups have begun to investigate the use of intraoperative ultrasound strain imaging in neurosurgery^{7,8,9}. Chakraborty *et al.* utilized a tracking system to track the tip of an ultrasound probe in order to help position the probe over a lesion before calculating a strain image. However, they did not present any quantitative data describing the accuracy with which their strain imaging system could localize a target. Another group used tracking of an ultrasound probe to help select RF frames for block-matching such that the movement between frames is primarily in the axial direction¹⁰. The tracking information in that case was used to improve the generation of quality elastograms, rather than to provide surgical guidance. To date, work to assess the ability of strain imaging to accurately localize surgical targets in a guidance setting remains relatively scarce.

The novel aspect of this paper is the merging of strain imaging with a tracking system to create a surgical guidance method which offers information not routinely available with any other intraoperative tool. The strain image plane was calibrated to the ultrasound probe such that strain images could be generated from the surgical field with automatic alignment to preoperative tomograms through tracking and registration. Co-registered strain images and tomograms were then directly compared to each other. A phantom study was performed to assess the ability of strain imaging to reconstruct the shape of a subsurface target, using contrast-enhanced CT and tracked B-mode image segmentation of the target for comparison.

2. METHODS

The ultrasound machine used in this study was an Acuson Antares with a VFX13-5 linear array transducer at 10 MHz and depth setting of 6 cm. The ultrasound was capable of standard B-mode imaging, as well as strain imaging through the commercial eSie Touch elasticity software module (Siemens Inc., Munich, Germany). Ultrasound data was tracked in 3D space by synchronizing the ultrasound video and tracking data using software based primarily on the Visualization Toolkit (VTK) on a host computer^{11,12}. The ultrasound video was captured by a Matrox Morphis Dual card (Matrox Imaging, Dorval, Canada), which recorded the analog video output of the ultrasound machine in real time. The ultrasound probe was tracked with a NDI Polaris (Northern Digital Inc., Waterloo, Canada) via the attachment of a passive optical target to the probe as shown in Figure 1.



Figure 1. The tracked ultrasound system consisted of a Polaris optical tracking system (a) and a passive target attached to the ultrasound probe (b).

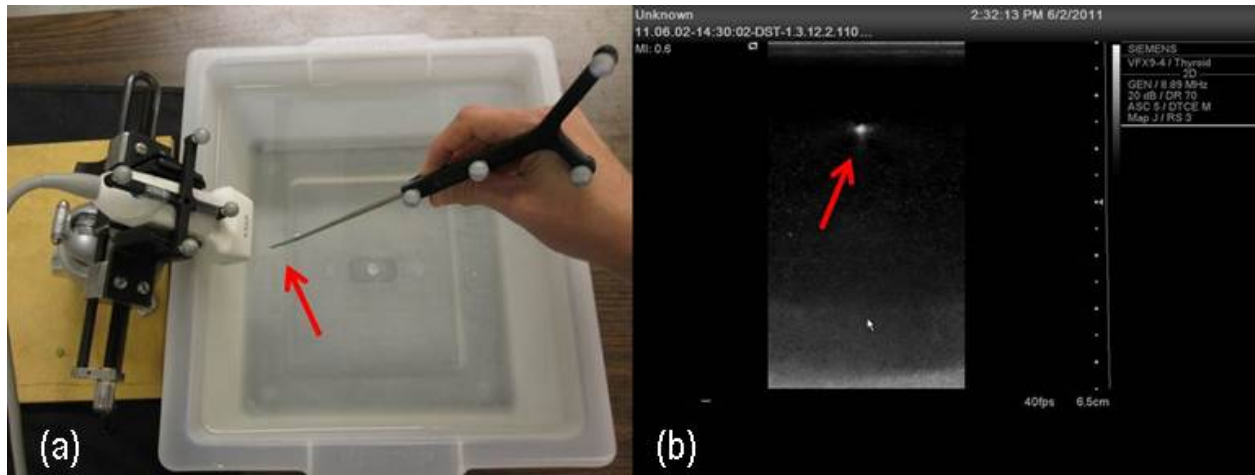


Figure 2. Calibration of the tracked ultrasound system. The ultrasound beam is approximated to be planar, and is sampled with a tracked pen probe (a) to produce bright corresponding points in the ultrasound images (b). A calibration transformation is computed which best matches the image points to the physical probe points.

The ultrasound images were calibrated for tracking by the method of Muratore *et al.* as shown in Figure 2, in which the ultrasound beam was approximated as a plane and was sampled with a tracked stylus to generate a calibration transformation which mapped from image space to physical space for each pixel in the images¹³. The combination of calibration and tracking matrices transformed each ultrasound image to a physical pose based on the pose of the ultrasound probe. The tracked ultrasound data could then be registered to preoperative images in the same manner as other intraoperative information, such as data from a tracked pen probe or laser range scanner¹⁴.

A phantom experiment was performed to assess the ability of tracked strain imaging to localize a subsurface target shape within a co-registered coordinate system with preoperative tomograms. To perform this study, four compliant polyvinyl alcohol (PVA) gel phantoms were constructed in an anthropomorphic organ-shaped mold, using a polyester sphere mock tumor doped with barium sulfate for CT contrast, and embedded glass beads in the surface to provide landmarks for registration¹⁵. The phantoms were fixed to a wooden base along with a tracked reference target. The phantoms were then each imaged with an xCAT ENT mobile CT scanner (Xoran Technologies, Ann Arbor, MI) at 640 x 640 x 356 with 0.4 mm isotropic voxels. The CT volumes were registered to physical space with a point-based registration using Horn's method and the surface beads localized with a tracked stylus and manually selected in the image volumes¹⁶. The bulk phantom and tumor were each segmented from the surrounding structures with Analyze 9.0 (Mayo Clinic, Rochester, MN) and the resulting segmentations were used to create digital surfaces with a standard marching cubes algorithm¹⁷. An example of one phantom with the CT tumor and co-registered ultrasound strain images is shown in Figure 3.

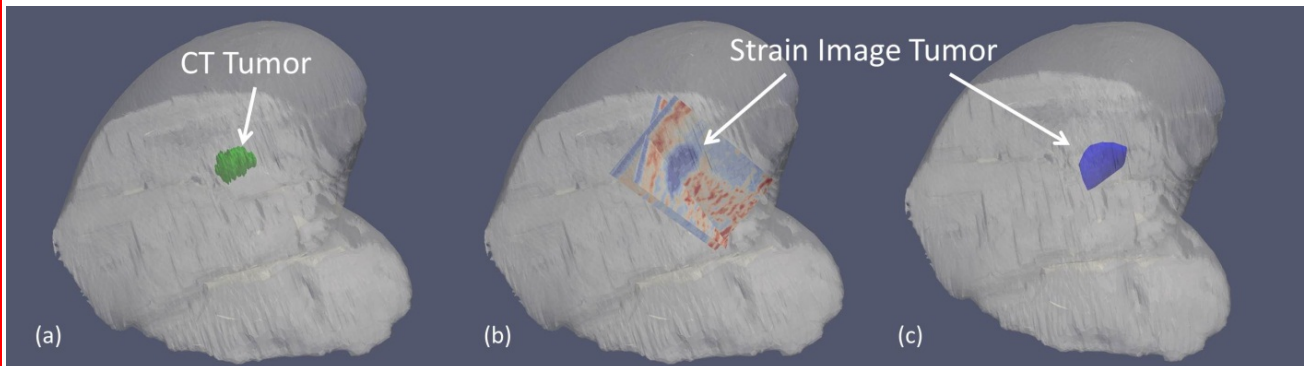


Figure 3. Embedded tumor surface generated from CT (a) and corresponding lesion shown in two roughly cross-sectional tracked strain images (b) and as a volume reconstructed from strain contours (c).

The phantoms were then imaged freehand using the tracked ultrasound probe at several positions above the subsurface target, with care taken to ensure that the probe was applied only in the axial direction for quality strain image generation. B-mode images were collected in a series of several swabs over the tumors. Strain images were collected incrementally with the probe at several angles, to minimize undesirable out-of-plane motion during strain image formulation. Each ultrasound acquisition lasted approximately 10 seconds. Lesion borders in each ultrasound image slice were segmented semi-automatically using a VTK implementation of the livewire technique based on Dijkstra's algorithm¹⁸. The segmentation resulted in a contour of points corresponding to the lesion border in B-mode and strain images. These points were then transformed to physical space using the ultrasound calibration from above. When a target was imaged from multiple points of view, tracking was used to place each border contour in its proper pose with respect to each other contour. Thus, the tracked strain images generated a point cloud which described the target shape based on the observed relative tissue stiffness. A volumetric representation of the point cloud was created by performing a 3D Delaunay triangulation of the contour points to produce a tetrahedral mesh¹⁹. The volume of the tumor mesh from B-mode and strain imaging was then compared to the volume of the CT tumor mesh.

3. RESULTS

The result of the point-based registration is shown in Figure 3. This figure shows the alignment of CT and tracked ultrasound images, as well as the ability of the strain imaging to localize the phantom tumor. Note that the borders of the strain image lesion were very well defined. The location and orientation of the strain images qualitatively displayed good agreement with the CT tumor as a result of the point-based registration done to align physical and CT space. The ability to accurately align ultrasound tumor borders with borders from preoperative imaging is a very important component of a tracked strain imaging system, and this aspect will be explored more thoroughly in a future work. The primary focus of this work was to assess the capability of a series of tracked strain image contours to generate a volume.

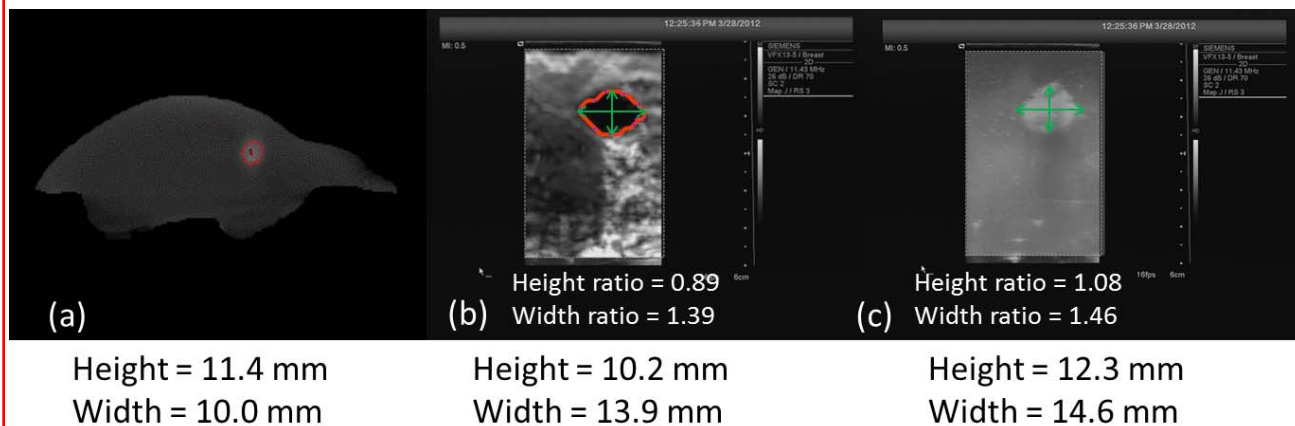


Figure 4. An example of the CT tumor dimensions (a), the corresponding strain tumor dimensions (b), and the B-mode tumor dimensions (c).

In order to reconstruct the shape of the phantom tumors, the borders of the lesions were extracted from contours segmented from tracked B-mode and strain images acquired from various positions above the target. Figure 4 shows an example of the tumor geometry in CT, strain imaging, and B-mode. For a quantitative comparison, the volume of the tumors in each phantom measured by each modality is shown below in Table 1.

Table 1. Results of geometric reconstruction of the phantom tumor volumes using CT, tracked B-mode images, and tracked strain images.

Phantom #	CT Volume (cm ³)	B-mode Volume (cm ³)	Strain Volume (cm ³)
1	1.17	1.50	1.70
2	2.25	1.77	1.50
3	1.98	1.59	2.39
4	1.01	1.95	1.90

The volume of the physical tumors during phantom construction was intentionally variable, and this was reflected in the segmented CT tumor volumes, which ranged from approximately 1.0 to 2.3 cm³. The volumes of the tumors reconstructed from tracked ultrasound contours were slightly different from the corresponding CT volumes, but were on the same order of magnitude and ranged from 1.5 to 2.4 cm³. In addition, the ultrasound-based volumes were typically more similar to each other than to the CT volume. This behavior was probably due to a combination of factors, particularly compression of the tissue by the ultrasound probe, as well as the scarcity of ultrasound border data compared to CT.

Table 2. Height-to-width ratios for the phantom tumor volumes from CT, B-mode reconstructions, and strain imaging reconstructions. Height and width were measured approximately through the tumor centroids.

Phantom #	CT Height/Width	B-mode Height/Width	Strain Height/Width
1	1.14	0.734	0.842
2	1.02	1.11	0.643
3	1.13	1.21	0.728
4	1.67	1.33	0.931

Height-to-width ratios for the phantom tumors were measured through the tumor centroids along axes defined by the CT slicing, and these results are shown in Table 2. The height-to-width ratio of the tumor in the strain-reconstructed tumor volumes showed a tendency to be smaller than either the CT or B-mode ratios. This could be partially attributed to compressional effects from the probe, as a certain level of pre-compression of the tissue was sometimes needed in order to generate proper tissue displacements for calculation of strain images. It should also be noted that although the CT in this case was considered the gold standard, the CT contrast enhancement of the tumor was imperfect due to uneven distribution of the contrast agent. This was verified using the B-mode images such as the example in Figure 4, which displayed a larger cross-sectional area than the CT through the tumor centroid. This uncertainty could be reduced or eliminated in the future by using a tumor manufactured with known dimensions with a machined mold.

4. CONCLUSIONS

We conclude that combining tracking data with ultrasound strain imaging is a feasible method of reconstructing the shape of a subsurface target. Given its unique contrast mechanism, tracked strain imaging shows promise as a complementary intraoperative data source for image-guided procedures. Future work will include further testing of the robustness of shape reconstruction in phantoms, as well as the development of novel methods which leverage the tracking system to correct for tissue displacement during strain imaging.

ACKNOWLEDGEMENTS

This work was supported by the National Institutes of Health–National Institute for Neurological Disorders and Stroke under Grant R01 NS049251-01A1, and by the National Institutes of Health award R01CA162477 from the National Cancer Institute.

REFERENCES

- [1] Burger, P. C., Heinz, E. R., Shibata, T. & Kleihues, P. "Topographic anatomy and CT correlations in the untreated glioblastoma multiforme". *J Neurosurg*, 68 (5), 698-704 (1988).
- [2] Van Den Hauwe, L., Parizel, P. M., Martin, J. J., Cras, P., Dedeyn, P. & Deschepper, A. M. A. "Postmortem Mri of the Brain with Neuropathological Correlation". *Neuroradiology*, 37 (5), 343-349 (1995).
- [3] Burns-Cox, N., Avery, N. C., Gingell, J. C. & Bailey, A. J. "Changes in collagen metabolism in prostate cancer: a host response that may alter progression". *J Urol*, 166 (5), 1698-1701 (2001).
- [4] Lee, H., Sodek, K. L., Hwang, Q., Brown, T. J., Ringuette, M. & Sodek, J. "Phagocytosis of collagen by fibroblasts and invasive cancer cells is mediated by MT1-MMP". *Biochem Soc Trans*, 35 (Pt 4), 704-706 (2007).
- [5] Doyley, M. M., Bamber, J. C., Fuechsel, F. & Bush, N. L. "A freehand elastographic imaging approach for clinical breast imaging: system development and performance evaluation". *Ultrasound Med Biol*, 27 (10), 1347-1357 (2001).
- [6] Konofagou, E. E., Harrigan, T. & Ophir, J. "Shear strain estimation and lesion mobility assessment in elastography". *Ultrasonics*, 38 (1-8), 400-404 (2000).
- [7] Chakraborty, A., Bamber, J. C. & Dorward, N. L. "Preliminary investigation into the use of ultrasound elastography during brain tumour resection". *Ultrasound*, 20 (1), 33-40 (2012).
- [8] Scholz, M., Lorenz, A., Pesavento, A., Brendel, B., Khaled, W., Engelhardt, M., Pechlivanis, I., Noack, V., Harders, A. & Schmieder, K. "Current status of intraoperative real-time vibrography in neurosurgery". *Ultraschall Med*, 28 (5), 493-497 (2007).
- [9] Selbekk, T., Brekken, R., Solheim, O., Lydersen, S., Hernes, T. A. N. & Unsgaard, G. "Tissue Motion and Strain in the Human Brain Assessed by Intraoperative Ultrasound in Glioma Patients". *Ultrasound in Medicine and Biology*, 36 (1), 2-10 (2010).
- [10] Rivaz, H., Foughi, P., Fleming, I., Zellars, R., Boctor, E. & Hager, G. "Tracked regularized ultrasound elastography for targeting breast radiotherapy". *Med Image Comput Assist Interv*, 12 (Pt 1), 507-515 (2009).
- [11] Boisvert, J., Gobbi, D., Vikal, S., Rohling, R., Fichtinger, G. & Abolmaesumi, P. "An Open-Source Solution for Interactive Acquisition, Processing and Transfer of Interventional Ultrasound Images". *The MIDAS Journal - Systems and Architectures for Computer Assisted Interventions* (2008).
- [12] Pace, D., Gobbi, D., Wedlake, C., Gumprecht, J., Boisvert, J., Tokuda, J., Hata, N. & Peters, T. "An open-source real-time ultrasound reconstruction system for four-dimensional imaging of moving organs". *Med Image Comput Assist Interv. MICCAI 2009* (2009).
- [13] Muratore, D. M. & Galloway, R. L. "Beam calibration without a phantom for creating a 3-D freehand ultrasound system". *Ultrasound in Medicine and Biology*, 27 (11), 1557-1566 (2001).
- [14] Pfeiffer, T. S., Simpson, A. L., Lennon, B., Thompson, R. C. & Miga, M. I. "Design and evaluation of an optically-tracked single-CCD laser range scanner". *Med Phys*, 39 (2), 636-642 (2012).
- [15] Fromageau, J., Gennisson, J. L., Schmitt, C., Maurice, R. L., Mongrain, R. & Cloutier, G. "Estimation of polyvinyl alcohol cryogel mechanical properties with four ultrasound elastography methods and comparison with gold standard testings". *IEEE Trans Ultrason Ferroelectr Freq Control*, 54 (3), 498-509 (2007).
- [16] Horn, B. K. P., Hilden, H. M. & Negahdaripour, S. "Closed-Form Solution of Absolute Orientation Using Orthonormal Matrices". *Journal of the Optical Society of America a-Optics Image Science and Vision*, 5 (7), 1127-1135 (1988).
- [17] Lorensen, W. E. & Cline, H. E. "Marching cubes: A high resolution 3D surface construction algorithm". *SIGGRAPH Comput. Graph.*, 21 (4), 163-169 (1987).
- [18] Dijkstra, E. W. "A note on two problems in connexion with graphs". *Numerische Mathematik*, 1 (1), 269-271 (1959).
- [19] Okabe, A., Boots, B. N. & Sugihara, K. o. [Spatial tessellations : concepts and applications of Voronoi diagrams]. (Wiley, 1992).